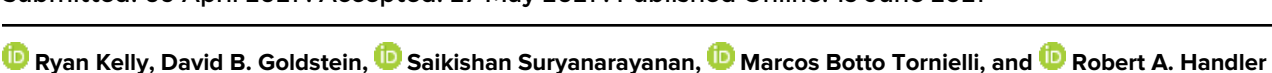
## The nature of bubble entrapment in a Lamb-Oseen vortex

Cite as: Phys. Fluids **33**, 061702 (2021); https://doi.org/10.1063/5.0053658 Submitted: 09 April 2021 . Accepted: 27 May 2021 . Published Online: 15 June 2021









iew Online/

Export Citation



Physics of Fluids
SPECIAL TOPIC: Tribute to
Frank M. White on his 88th Anniversary



# The nature of bubble entrapment in a Lamb-Oseen vortex

Cite as: Phys. Fluids **33**, 061702 (2021); doi: 10.1063/5.0053658 Submitted: 9 April 2021 · Accepted: 27 May 2021 ·

Published Online: 15 June 2021

Ryan Kelly, 🛅 🕞 David B. Goldstein, Saikishan Suryanarayanan, 🕞 Marcos Botto Tornielli, 🕞 and Robert A. Handler 🕞









University of Texas at Austin, Austin, Texas 78712, USA

#### **ABSTRACT**

Bubble trajectories in the presence of a decaying Lamb-Oseen vortex are calculated using a modified Maxey-Riley equation. Some bubbles are shown to get trapped within the vortex in quasi-equilibrium states. All the trapped bubbles exit the vortex at a time that is only a function of the Galilei number and the vortex Reynolds number. The set of initial bubble locations that lead to entrapment is numerically determined to show the capturing potential of a single vortex. The results provide insight into the likelihood of bubble entrapment within vortical structures in turbulent flows.

Published under an exclusive license by AIP Publishing. https://doi.org/10.1063/5.0053658

Understanding the dynamics of particle motion in fluid flows is required for a wide variety of applications. These include predicting particle motion in the environment as well as flows of engineering interest.<sup>1,2</sup> One particular case of interest is that of wall-bounded turbulent flows in which small particles or bubbles are used to modify coherent drag-producing structures.3-7 Recently, this has been simulated via direct numerical simulations with promising results for light particles suppressing isotropic turbulence,8 along with large eddy simulations showing turbulent drag reduction via bubbles in channel and boundary layer flows. In this study, we wish to uncover the physics of how a small bubble moves in the presence of a vortex as a step toward understanding the complex dynamics of bubbles in turbulence. It has been shown that bubbles can be attracted to the center of a single vortex, 10-12 which is significant because it can provide an opportunity to target and control vortical structures in turbulence. In the present study, we show that bubble motion through a vortex that diffuses over time, which is a better representation of an evolving vortex in a turbulent flow, can lead to interesting features such as selective entrapment.

The problem of bubble or light particle tracking is not a new one, and many aspects have been studied rigorously over the past several decades. <sup>13</sup> There are now many sophisticated multiphase flow solvers and bubble-tracking methods, such as level-set and front tracking methods, <sup>14–16</sup> for a wide range of bubble sizes, which include bubble deformation. However, we study a simplified vortex model for a point particle to examine the basic principles of a single bubble's behavior near a vortex. A direct numerical simulation of turbulent flow with a

large number of bubbles provides statistical information that can be challenging to interpret, and point particle models are at least qualitatively similar. Furthermore, the potential dependence of the results on a large number of parameters present in such a problem makes it difficult to obtain broad scientific insight which a simple model like ours can provide. Real turbulent vortical structures are 3D and continuously break and merge, but the present Lamb–Oseen vortex model, in particular, is useful because it is an exact solution to the Navier–Stokes equations, which provides a tractable framework to understand how bubbles behave in the presence of vortices. It also includes one effect of flow unsteadiness due to the realistic vortex diffusion, and this feature may provide useful insight into the potential entrapment of bubbles by transient vortical structures in a turbulent flow.

The modified Maxey–Riley equation for a 2D bubble with lift in the x–y plane is given by  $^{18}$ 

$$\frac{d\mathbf{v}}{dt} = 3\frac{D\mathbf{u}}{Dt} + \frac{1}{\tau_L}(\mathbf{u} - \mathbf{v}) + (\mathbf{u} - \mathbf{v}) \times \boldsymbol{\omega} - 2\mathbf{g},\tag{1}$$

where  ${\bf u}$  is the fluid velocity,  ${\bf v}$  is the bubble velocity,  ${\bf \omega}$  is the fluid vorticity,  ${\bf g}$  is gravity, and  $\tau_b \equiv a^2/(6\nu)$  is the so-called "bubble response time," defined as the time it takes for the bubble to reach  $\approx$ 63% of its terminal velocity when released from rest. Here, we consider cases that are in the microbubble regime. Therefore, we may assume that the bubble does not deform and acts as a point particle with zero mass and perfect slip at the surface–fluid interface. Additionally, we model the flow field,  ${\bf u}$ , as a Lamb–Oseen line vortex in the z-direction, which

<sup>&</sup>lt;sup>2</sup>George Mason University, 4400 University Dr, Fairfax, Virginia 22030, USA

a) Author to whom correspondence should be addressed: ryankellybp11@gmail.com

has a core radius of  $r^* = 2.2418\sqrt{\nu t}$ , <sup>19</sup> assumed to be much larger than the radius of the bubble.  $\frac{d\mathbf{v}}{dt}$  is the acceleration of the bubble, whereas  $\frac{D\mathbf{u}}{Dt}$  is the material derivative of the fluid velocity and represents added mass effects. The next terms in Eq. (1) represent Stokes' drag, lift due to vorticity, and buoyancy, respectively. This simplified model is relevant to bubbles in a turbulent boundary layer and is consistent with the observed bubble motion. <sup>4–6</sup>

It is more convenient to non-dimensionalize Eq. (1) by scaling length with the bubble radius, a, and time by the bubble response time. Doing this and scaling gravity by some characteristic acceleration,  $g_0$ , gives

$$\frac{d\mathbf{V}}{d\tau} = 3\frac{D\mathbf{U}}{D\tau} + (\mathbf{U} - \mathbf{V}) + (\mathbf{U} - \mathbf{V}) \times \mathbf{\Omega} - \frac{Ga}{18}\mathbf{G},\tag{2}$$

where the capital letters represent non-dimensional forms of the respective variables in Eq. (1) and  $\tau$  is a non-dimensional time. Ga is the Galilei number, a non-dimensional parameter defined as  $Ga \equiv g_0 a^3/\nu^2$ , where  $\nu$  is the kinematic viscosity. This can be understood intuitively as the ratio of buoyant forces to viscous forces. The non-dimensional velocity field for a Lamb–Oseen vortex in the  $\xi - \eta$  plane is given by

$$\mathbf{U} = \left[ -\frac{Re_v}{12\pi} \frac{\eta}{\xi^2 + \eta^2} \left( 1 - \exp\left( -\frac{3(\xi^2 + \eta^2)}{2\tau} \right) \right) \right] \mathbf{e}_{\xi}$$

$$+ \left[ \frac{Re_v}{12\pi} \frac{\xi}{\xi^2 + \eta^2} \left( 1 - \exp\left( -\frac{3(\xi^2 + \eta^2)}{2\tau} \right) \right) \right] \mathbf{e}_{\eta}, \quad (3)$$

and the vorticity is given by

$$\mathbf{\Omega} = \frac{Re_v}{4\pi\tau} \exp\left(-\frac{3(\xi^2 + \eta^2)}{2\tau}\right) \mathbf{e}_{\zeta},\tag{4}$$

where  $\xi$ ,  $\eta$ , and  $\zeta$  replace x, y, and z as non-dimensional coordinates, respectively.  $Re_v$  is the vortex Reynolds number defined as  $Re_v \equiv \Gamma/\nu$  and is a measure of vortex strength relative to the fluid viscosity, where  $\Gamma$  is the circulation. We solve this system of differential equations numerically using the ode45 function in MATLAB (R2020a) with stringent convergence criteria (the relative tolerance is set to  $10^{-9}$  and the absolute tolerance is set to  $10^{-11}$  to ensure all features of the trajectories are accurately resolved).

We first consider the case of a bubble released from  $\eta = -75$  at various  $\xi$  values at time  $\tau = 350$  and initially rising at terminal velocity. The solution of Eq. (2) in this case shows a general trend of bubbles being attracted to the vortex core, shown in Fig. 1, with trajectories similar to those found in the simulations and experiments in Refs. 10 and 11. For a vortex of a given radius and circulation, it can be shown 12,20,21 that there is a point where all forces acting on the bubble are in equilibrium, and the bubble can be trapped. The present simulations, however, involve a vortex whose radius increases with time as a result of viscous diffusion. Therefore, the equilibrium point slowly moves outward before ceasing to exist, resulting in a quasi-equilibrium state. If a bubble is drawn into the core and achieves this quasiequilibrium state, it may be considered "captured" by the vortex. Its trajectory first displays a rapid periodic spiraling inside the core before reaching quasi-equilibrium. At a certain point, the bubble escapes the pull of the vortex and continues moving upward. The details of the spiraling motion are affected by the physical properties of the flow and

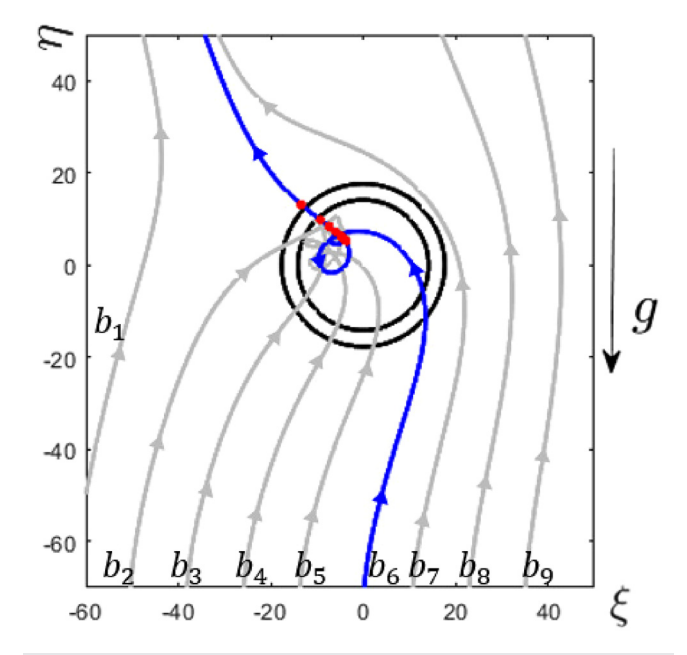


**FIG. 1.** Example trajectories of bubbles  $(b_1-b_9)$  with  $Re_v=10\,000$ , Ga=-240, released from  $\eta_0=-75$  at  $\tau_0=350$  and initially at terminal rise velocity. Paths  $b_2-b_6$  are all trapped bubble trajectories. A few equilibrium points are plotted (red dots) along with the vortex core at the release and exit times,  $\tau_0$  and  $\tau_{exit}$  (black).

bubble as well as the initial conditions; however, the quasi-equilibrium motion only depends on the constant physical properties. That is, if the bubble is released early (relative to vortex inception) near the center of the vortex, where its strength is large, the bubble will spiral many more times before reaching the quasi-equilibrium state compared to a similar bubble released later or farther away. However, once the bubble reaches equilibrium, the trajectory is identical to that of any other captured bubble, regardless of where or when it starts. In the example shown in Fig. 1, the gray lines of captured bubble trajectories  $(b_2 - b_5)$  collapse onto the highlighted trajectory  $(b_6)$  around the location of the first few equilibrium points shown.

The quasi-equilibrium state is particularly interesting. Since the bubble velocity and acceleration are very small in that state, Eq. (2) can be solved under the assumptions that  $\mathbf{V} = \frac{d\mathbf{V}}{d\tau} = \mathbf{0}$  to determine positions at each time where the bubble satisfies the equilibrium condition. The instantaneous equilibrium point, however, continually moves outward with the bubble following suit during this phase of motion, as illustrated in the example shown in Fig. 1. Figure 2 shows the bubble speed and the forces acting in the  $\eta$ -direction on the bubble vs time, which reveals that the time spent in equilibrium is much longer than the time spent initially spiraling. In this example, the bubble is released just below the vortex core at  $\tau = 350$  and spirals rapidly until about  $\tau \approx 370$  where it remains in quasi-equilibrium until  $\tau \approx 490$  when it escapes and returns to (a different) equilibrium as it rises upward at terminal velocity. The shape of the trajectory will vary with physical parameters and initial conditions, but all trapped trajectories exhibit the same qualitative behavior in which there is some brief period of spiraling when the bubble reaches the vortex core before it settles into the quasi-equilibrium state, for what can be a

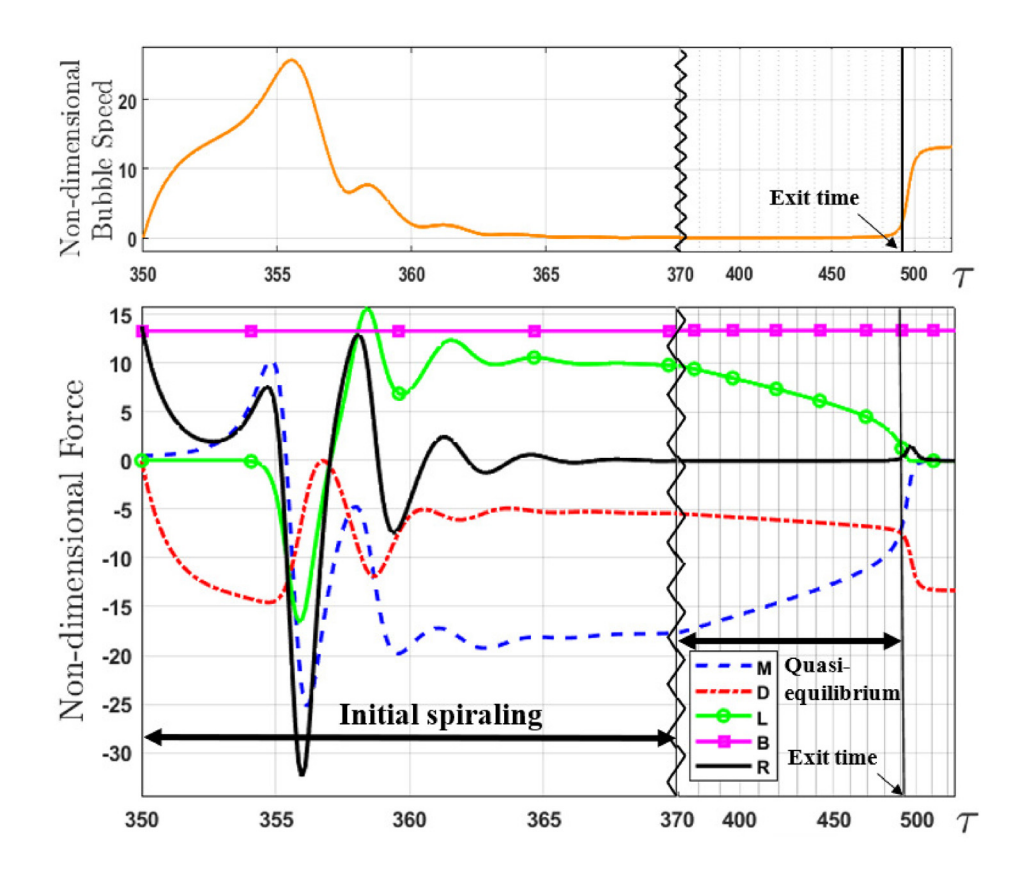


**FIG. 2.** (Top) Bubble speed vs time for a bubble captured by a vortex with  $Re_v=10\,000,~Ga=-240,~$  released from  $(\xi_0,\eta_0)=(0,-75)$  at  $\tau_0=350.$  (Bottom)  $\eta$ -component of forces acting on the bubble over time as it passes through the vortex core. M= added mass effects, D= drag, L= lift, B= buoyancy, R= resultant force. Note the change in time spacing starting at  $\tau=370,~$  denoted by the wavy line.

much longer duration, until it escapes. Although these equilibrium points are useful for locating where a bubble will nearly come to rest, it should be noted that bubble entrapment is assumed, and its existence does not guarantee a given bubble will be trapped. The equilibrium points are determined solely based on  $\tau$ ,  $Re_v$ , and Ga, and are the same irrespective of the bubble's initial position.

While the duration of entrapment is difficult to determine precisely, it can be estimated quite well from the  $Re_v$ , Ga, and initial conditions, which are known a priori. The time at which the bubble enters the vortex can be estimated based on the bubble rise speed in a still fluid:  $\tau_{ent} = 18\eta_0/Ga$ , where  $\eta_0$  is the  $\eta$  position of the bubble at the time it is released. The exit time ( $\tau_{exit}$ ) can be estimated by solving a special case of Eq. (2). Using what we found by analyzing the bubble's quasi-equilibrium state, the bubble escapes the vortex at the last time an equilibrium point exists. While this particular point cannot be found analytically, a nearby one can be: the point at which the equilibrium position and the vortex core radius are equivalent. We can take the bubble's distance from the origin,  $\sqrt{\xi^2 + \eta^2}$ , to be the same as the core radius at the estimated exit time. Using the scaling variables,  $\tau = t/\tau_b$  and  $r = r^*/a$ , we can convert the core radius of the Lamb–Oseen vortex to nondimensional form,

$$r = \frac{r^*}{a} = \frac{2.2418}{a} \sqrt{\nu \frac{6a^2}{\nu} \tau} = 0.9152 \sqrt{\tau}.$$
 (5)

Thus, we assume  $r_{core} = 0.9152\sqrt{\tau_{exit}}$ . We substitute this into Eqs. (3) and (4) along with the polar representations,  $\xi = r \cos \theta$  and

 $\eta=r\sin\theta$ , where  $\theta$  is the angle measured counterclockwise from the positive  $\xi$ -axis. Given the assumption  $r=r_{core}$  and equilibrium conditions, Eq. (2) is simplified enough to be solved analytically based solely on  $Re_v$  and Ga (the solution process is shown in detail in the supplementary material). Consequently, any trapped bubbles with the same  $Re_v$  and Ga will have identical estimated exit times, regardless of initial conditions, due to the vortex diffusing at a rate independent of the bubble's effects. This is not the case for two-way coupling simulations, and  $\tau_{exit}$  varies since the bubble disturbs the vortex,  $^{12}$  thereby reducing the crucial added mass force necessary for entrapment.

We can define the bubble as "trapped" when it spends at least a certain amount of time,  $\Delta \tau_{crit}$ , in the core. The results are robust with respect to the choice of  $\Delta \tau_{crit}$ , provided  $\Delta \tau_{crit} \ll \tau_{exit} - \tau_{ent}$ . A "capture" region can then be determined by simulating bubbles from different initial positions to determine which ones are trapped. A few examples of these capture regions are shown in Fig. 3, where any bubble released inside the boundaries will be captured by the vortex for a duration of at least  $\Delta \tau_{crit} = 50$ . The capture regions in Fig. 3 were determined using a bubble release time of  $\tau_0 = 1$ , but it was found that the choice of  $\tau_0$  only altered the bottom location of the capture region, and features near the vortex core were unchanged.

The width and inclination of these fingerlike capture regions vary with the physical parameters: larger  $Re_v$  and smaller Ga tend to expand and rotate the region, whereas a smaller  $Re_v$  and larger Ga tend to shrink and straighten it. This aligns with physical intuition where a higher Ga indicates a stronger buoyant force, meaning bubbles further away from the core (in the direction normal to the

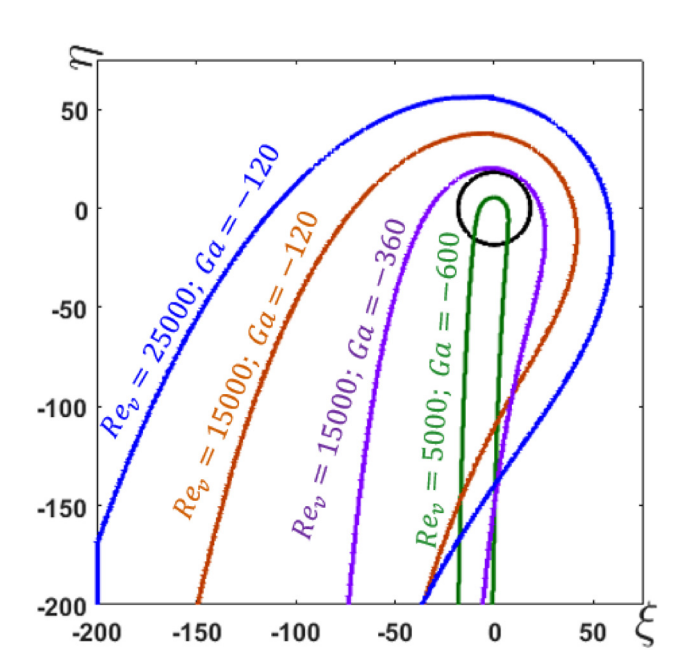


**FIG. 3.** Capture regions for various  $Re_v$  and Ga. The black circle represents the vortex core at  $\tau = 500$ .

buoyant force) are less likely to be captured. On the other hand, a higher  $Re_v$  indicates a stronger vortex with higher pressure gradients, pushing the bubble toward the core. Bubbles more directly opposing the direction of fluid will naturally slow down and are more likely to be trapped. Therefore, bubbles to the left of a counterclockwise-rotating vortex will be favored for entrapment. These regions may extend very far downward and can be estimated by the relation  $\eta_{bottom} = \frac{Ga}{18} (\tau_{exit} - \tau_0 - \Delta \tau_{crit})$ . For perspective, a vortex in water with  $Re_v = 10\,000$  and a bubble with a radius of 1 mm may have a capture region, which extends several meters below the vortex core.

Although the capture region is well-defined for smaller values of  $Re_v$  and Ga, the simple shape can break down and produce multiple tails when these values are large enough, as shown in the examples of Fig. 4. Increasing  $Re_v$  and Ga first produces a single narrow streak of initial points where bubbles are not trapped within the fingerlike shape; increasing parameters further produces additional streaks and widens them until no points can be captured (see the supplementary material for more examples). These streaks arise due to the bubble accelerating too quickly near the core and passing by it instead of being captured. The chaotic nature of the system means that the location, number, and width of these streaks are interesting but difficult to predict.

The present simulations reveal the complex dynamics of bubbles in the presence of vortices, even for the simple but well-defined setting of a non-deformable bubble rising through a decaying Lamb-Oseen vortex. The results from the simple model considered here are not intended to be directly applicable to realistic situations involving turbulent flows, but they provide insights into bubble entrapment by vortices that could be of general relevance as well as reveal interesting features such as chaotic entrapment patterns. While there is broad agreement with earlier work that bubbles are generally attracted to the

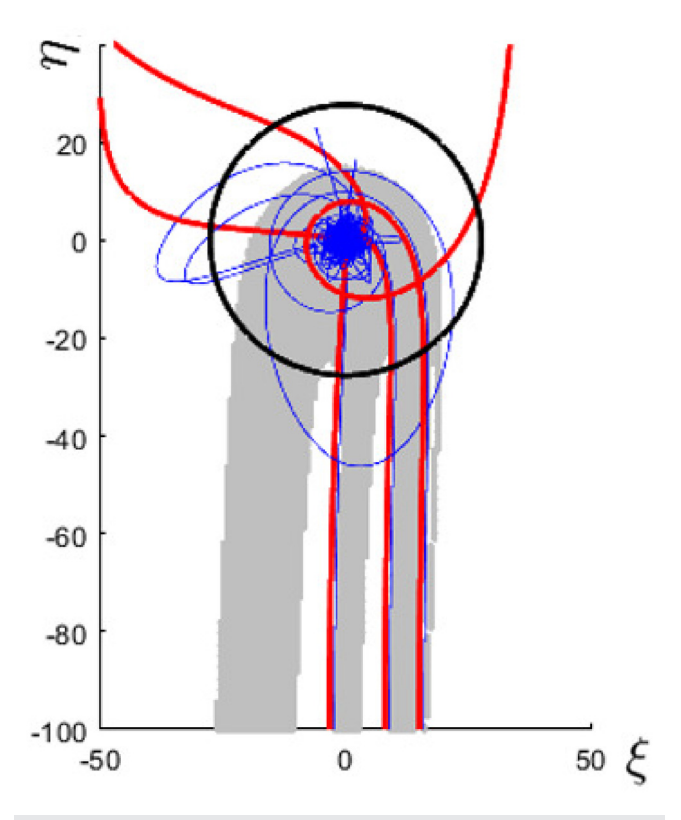


**FIG. 4.** Capture region (shaded) for  $Re_v = 75\,000$  and Ga = -3600. Example escaped trajectories are plotted in bold (red) and adjacent trapped trajectories are plotted as thin lines (blue).

vortex core, we have discovered the existence of quasi-equilibrium points in the decaying vortex that can temporarily "trap" the bubbles within the vortex. Any trapped bubble is observed to exit the vortex at a time when the vortex has no theoretical equilibrium point [that is, when Eq. (2) under equilibrium assumptions has no solution]. Thus, a method for a priori estimation of the duration of a bubble's entrapment is demonstrated in this work. Bubble entrapment is also observed to be practically binary, in the sense that a bubble is either trapped or it is not. Trapped bubbles may take over two orders of magnitude longer to rise through the computational domain considered here than bubbles that are not trapped (details in the supplementary material). This is significant from the point of view of flow control as the residence time of a bubble is likely to be related to its ability to alter the vortex. 12 The present results also analyze how the "capture region" varies with the parameters of the problem. This is again significant for flow control applications that rely on bubbles released from outside the vortex, which eventually enter and alter the vortex. This region was found to be finger-shaped, where the finger's width and curvature depend on  $Re_v$  and Ga, and we provide an explanation for the observed dependence.

Interestingly, for large values of Ga relative to  $Re_v$ , it is found that some bubbles released from within the finger-shaped boundary actually evade capture. That is, two bubbles that are initially very close to each other can have divergent trajectories in the neighborhood of the vortex: one of them proceeding to reside within the vortex core for a

long time, while the other slips past the vortex. This observation is consistent with chaotic nature of this parameter regime resulting from relatively small stabilizing viscous effects compared to the other forces acting on the bubble. Further analysis shows that the loci of all bubble initial points which lie within the overall finger-shaped boundary of the capture region but evade capture appear as a series of long streaks. The width and number of these streaks vary depending on the physical parameters. Example cases of capture regions, the bubble trajectories in the chaotic regime, and bubble rise times are shown in the supplementary material. The findings on the duration of bubble entrapment and capture regions are particularly useful for flow control strategies involving bubbles, such as suppression of shear layer growth and drag reduction through the disruption of hairpin vortices in a turbulent boundary layer.

#### **SUPPLEMENTARY MATERIAL**

See the supplementary material for further details. This includes two videos demonstrating how a bubble moves through a Lamb–Oseen vortex with emphasis on the forces and the equilibrium points. Furthermore, there is a description of the non-dimensionalization process in detail, a detailed analysis of bubble exit conditions, and further discussion of capture region features including several figures.

We gratefully acknowledge the support of the National Science Foundation through Award Nos. 1905288 and 1904953.

#### **DATA AVAILABILITY**

The data that support the findings of this study are available from the corresponding author upon reasonable request.

### **REFERENCES**

- <sup>1</sup>G. T. Csanady, *Turbulent Diffusion in the Environment* (D. Reidel Publishing Company, Dordrecht/Boston, 1973).
- <sup>2</sup>A. Guha, "Transport and deposition of particles in laminar and turbulent flow," Annu. Rev. Fluid Mech. 40, 311–341 (2008).
- <sup>3</sup>M. R. Maxey and J. J. Riley, "Equations of motion for a small rigid sphere in a nonuniform flow," Phys. Fluids 26, 883–889 (1983).

- <sup>4</sup>L.-P. Wang and M. R. Maxey, "The motion of microbubbles in a forced isotropic and homogeneous turbulence," Appl. Sci. Res. 51, 291–296 (1993).
- <sup>5</sup>P. D. M. Spelt and A. Biesheuvel, "On the motion of gas bubbles in homogeneous isotropic turbulence," J. Fluid Mech. **336**, 221–244 (1997).
- <sup>6</sup>J. Xu, M. Maxey, and G. Karniadakis, "Numerical simulation of turbulent drag reduction using micro-bubbles," J. Fluid Mech. 468, 271–281 (2002).
- <sup>7</sup>K. Sene, J. Hunt, and N. Thomas, "The role of coherent structures in bubble transport by turbulent shear flows," J. Fluid Mech. 259, 219–240 (1994).
- <sup>8</sup>K. Luo, Z. Wang, D. Li, J. Tan, and J. Fan, "Fully resolved simulations of turbulence modulation by high-inertia particles in an isotropic turbulent flow," Phys. Fluids **29**, 113301 (2017).
- <sup>9</sup>X. Zhang, J. Wang, and D. Wan, "Euler-Lagrange study of bubble drag reduction in turbulent channel flow and boundary layer flow," Phys. Fluids 32, 027101 (2020).
- <sup>10</sup>E. van Nierop, S. Luther, J. Bluemink, J. Magnaudet, A. Prosperetti, and D. Lohse, "Drag and lift forces on bubbles in a rotating flow," J. Fluid Mech. 571, 439–454 (2007).
- <sup>11</sup>N. H. Thomas, T. R. Auton, K. Sene, and J. C. R. Hunt, "Entrapment and transport of bubbles by plunging water," in *Gas Transfer at Water Surfaces*, edited by W. Brutsaert and G. H. Jirka (Springer, Dordrecht, The Netherlands, 1984), pp. 255–268.
- <sup>12</sup>E. Climent and J. Magnaudet, "Dynamics of a two-dimensional upflowing mixing layer seeded with bubbles: Bubble dispersion and effect of two-way coupling," Phys. Fluids 18, 103304 (2006).
- <sup>13</sup>V. Mathai, D. Lohse, and C. Sun, "Bubbly and buoyant particle-laden turbulent flows," Annu. Rev. Condens. Matter Phys. 11, 529–559 (2020).
- <sup>14</sup>F. Gibou, R. Fedkiw, and S. Osher, "A review of level-set methods and some recent applications," J. Comput. Phys. 353, 82–109 (2018).
- <sup>15</sup>G. Tryggvason, B. Bunner, A. Esmaeeli, D. Juric, N. Al-Rawahi, W. Tauber, J. Han, S. Nas, and Y.-J. Jan, "A front-tracking method for the computations of multiphase flow," J. Comput. Phys. 169, 708–759 (2001).
- <sup>16</sup>G. Tryggvason and J. Lu, "Multifluid flows in a vertical channel undergoing topology changes," Phys. Rev. Fluids 4, 084301 (2019).
- <sup>17</sup>A. Loisy and A. Naso, "Interaction between a large buoyant bubble and turbulence." Phys. Rev. Fluids 2, 014606 (2017).
- <sup>18</sup>I. M. Mazzitelli, D. Lohse, and F. Toschi, "On the relevance of the lift force in bubbly turbulence," J. Fluid Mech. 488, 283–313 (2003).
- 19 P. K. Kundu, I. M. Cohen, and D. R. Dowling, "Kinematics," in Fluid Mechanics 6th ed (Fleevier 2016) Chap 3 pp. 77-108
- Mechanics, 6th ed. (Elsevier, 2016), Chap. 3, pp. 77–108.
  Lasheras and K.-K. Tio, "Dynamics of a small spherical particle in steady two-dimensional vortex flows," Appl. Mech. Rev. 47, S61–S69 (1994).
- <sup>21</sup>G. R. Ruetsch and E. Meiburg, "On the motion of small spherical bubbles in two-dimensional vortical flows," Phys. Fluids A 5, 2326–2341 (1993).